1090 *Inorg. Chem.* **1995,** *34,* 1090−1093

Synthesis and Electrochemistry of Mo[BH(Me$_2$pz)$_3$](NO)[S(CH$_2$)$_2$CONH(CH$_2$)$_2$S]† as a Probe of the Effects of N−H···S Hydrogen Bonding on Redox Potentials

Jiong Huang,[‡] Robert L. Ostrander,[§] Arnold L. Rheingold,[§] and Marc Anton Walters*,[‡]

Departments of Chemistry, New York University, New York, New York 10003, and
University of Delaware, Newark, Delaware 19716

Received October 20, 1994[®]

A series of bidentate alkanethiolate compounds Mo[BH(Me$_2$pz)$_3$](NO)[SRS], [SRS]$^{2-}$ = [S(CH$_2$)$_2$CONH(CH$_2$)$_2$S]$^{2-}$ (**1**), [S(CH$_2$)$_5$S]$^{2-}$ (**2**), and [S(CH$_2$)$_6$S]$^{2-}$ (**3**), have been synthesized in order to determine the effects of N−H···S hydrogen bonding on redox potentials in metal−thiolate complexes. Complex **1** was structurally characterized by X-ray crystallography. It crystallizes in the space group $P2_1/c$ with a = 11.878(2) Å, b = 10.8040(10) Å, c = 21.453(4) Å, α = 90°, β = 105.54°, γ = 90°, V = 2652.4(7) Å^3, Z = 4, and R = 0.0374. Redox potentials of −0.793 V (**1**), −0.930 V (**2**), and −1.013 V (**3**) (relative to SCE) were measured in CH$_3$CN by cyclic voltammetry. A comparison of complexes **1**−**3** by solution vibrational spectroscopy shows that the high redox potential of **1** may be attributed to the presence of N−H···S hydrogen bonds. The nitrosyl stretching frequency, ν(NO), was assigned in the resonance Raman spectra of complexes **1**−**3**. This band decreased in frequency in parallel with the decrease in redox potential. For complex **1** in solution the values of the amide N−H stretching frequency, ν(NH), 3434 and 3308 cm^{-1} indicates a hydrogen bonding equilibrium constant of K = [NH$_{\text{bonded}}$]/[NH$_{\text{free}}$] = 6.7.

Introduction

The investigation of H-bonding and charge−dipole or dipole−dipole interactions is necessary for an understanding of active site characteristics in electron transfer metalloproteins.[1−4] A recognition of this need is evident in the many studies of the structural and redox effects of N−H···S hydrogen bonds in Fe−S protein model compounds.[5−10] Until recently, N−H···S hydrogen bonds between ligated *alkane*thiolate sulfur and neighboring amide groups had been observed by crystallography only in proteins. In structurally-characterized model compounds, the occurrence of stable N−H···S hydrogen bonds in solution was substantiated only in complexes with rigid *benzene*thiolate ligands with ortho N−H groups.[5,7,8]

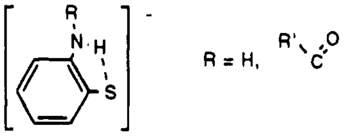

Redox potentials in such complexes are likely to be influenced both by N−H···S hydrogen bonding and substituent inductive effects, which act through a π-p$_\pi$ orbital pathway.

Recently, we reported on two Mo−hydrotris(pyrazolyl)borate alkanethiolate complexes with the formula Mo[HB(Me$_2$pz)$_3$](NO)(SR)$_2$ that incorporate the mercapto amide ligands [SR]$^-$ = [S(CH$_2$)$_n$CONHCH$_3$]$^-$, n = 1 and 2.[11−13] In these complexes, N−H···S bond formation was observed for the shorter of the two ligands, [S(CH$_2$)CONHCH$_3$]$^-$, which cyclizes to form a five-membered ring.

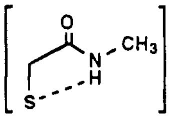

In a new approach, we have expanded on the chemistry of bidentate thiolate complexes[14,15] Mo[BH(Me$_2$pz)$_3$](X)(SRS) in the study of N−H···S hydrogen bonding and its effect on redox potential. In what follows, the structural and electronic properties are discussed for a series of complexes Mo[BH(Me$_2$pz)$_3$](NO)[S(CH$_2$)$_2$CONH(CH$_2$)$_2$S] (**1**) and Mo[BH(Me$_2$pz)$_3$](NO)[S(CH$_2$)$_n$S], n = 5 (**2**) and 6 (**3**). In solution, the amide group of complex **1** forms an intraligand N−H···S hydrogen bond with coordinated sulfur. The amide group is, in essence, strapped to the complex, thereby enforcing an amide−sulfur proximity that nearly assures the formation of N−H···S

[†] (N-(2-mercaptoethyl)-2′-mercaptopropionamido)(nitrosyl)[hydrotris(3,5-dimethyl-1-pyrazolyl)borato]molybdenum.

[‡] New York University

[§] University of Delaware.

[®] Abstract published in *Advance ACS Abstracts,* February 1, 1995.

(1) Walters, M. A.; Dewan, J. C.; Min, C.; Pinto, S. *Inorg. Chem.* **1991**, *30*, 2656−2662.

(2) Langen, R.; Jensen, G. M.; Jacob, U.; Stephens, P. J.; Warshel, A. *J. Biol. Chem.* **1992**, *267*, 25625−25627.

(3) Backes, G.; Mino, Y.; Loehr, T. M.; Meyer, T. E.; Cusanovich, M. A.; Sweeney, W. V.; Adman, E. T.; Sanders-Loehr, J. *J. Am. Chem. Soc.* **1991**, *113*, 2055−2064.

(4) Hill, C. L.; Renaud, J.; Holm, R. H.; Mortenson, L. E. *J. Am. Chem. Soc.* **1977**, *99*, 2549−2557.

(5) Huang, J.; Dewan, J. C.; Walters, M. A. *Inorg. Chim. Acta* **1995**, *228*, 199−206.

(6) Ueyama, N.; Nakata, M.; Fuji, M.-A.; Tetrakawa, T.; Nakamura, A. *Inorg. Chem.* **1985**, *24*, 2190−2196.

(7) Ueyama, N.; Okamura, T.-A.; Nakamura, A. *J. Am. Chem. Soc.* **1992**, *114*, 8129−8137.

(8) Ueyama, N.; Okamura, T.-A.; Nakamura, A. *J. Chem. Soc., Chem. Commun.* **1992**, 1019−1020.

(9) Nakamura, A.; Ueyama, N. In *Metal Clusters in Proteins*; Que, L., Ed.; American Chemical Society: Washington, DC, 1988; Chapter 14.

(10) Nakamura, A.; Ueyama, N.; Okamura, T.-A.; Takamizawa, S. *J. Inorg. Biochem.* **1993**, *51*, 30.

(11) Huang, J.; Walters, M. A. *J. Inorg. Biochem.* **1993**, *51*, 24.

(12) Huang, J.; Ostrander, R. L.; Rheingold, A. L.; Leung, Y.; Walters, M. A. *J. Am. Chem. Soc.* **1994**, *116*, 6769−6776.

(13) Reynolds, S. J.; Smith, C. F.; Jones, C. J.; McCleverty, J. A. *Inorg. Synth.* **1983**, *23*, 4−9.

(14) Trofimenko, S. *Chem. Rev.* **1993**, *93*, 943−980.

(15) Chang, C. S. J.; Collison, D.; Mabbs, F. E.; Enemark, J. H. *Inorg. Chem.* **1990**, *29*, 2261−2267.

0020-1669/95/1334-1090$09.00/0

hydrogen bonds. Complexes of this type are well suited for the investigation of noncovalent interactions that influence redox characteristics of electron transfer metalloproteins.

Experimental Section

All reactions, unless otherwise specified, were carried out in dry, oxygen-free solvents under nitrogen. Silica gel G, 10−40 μm, was used with 10% THF in CH_2Cl_2 as the eluant for column chromatography.

HS(CH$_2$)$_2$CONH(CH$_2$)$_2$SH. Cysteamine, $HS(CH_2)_2NH_2$ (9.15 g, 119 mmol), and ethyl 3-mercaptopropionate (7.96 g, 59 mmol) were combined in degassed anisole (60 mL), and the solution was refluxed for 7 h. The solvent and excess cysteamine were evaporated under vacuum on a hot water bath. The unreacted ethyl mercaptopropionate was extracted with petroleum ether (bp 35−60 °C, 100 mL). The remaining cysteamine was removed by vacuum sublimation, leaving the product as a colorless liquid (2.0 g, 20.5%). IR (neat liquid, cm^{-1}): 1651.6 (CO), 2552.2 (SH). IR ($CDCl_3$, cm^{-1}) (4.0 mM): 3448 $(N-H)_{free}$ and 3333 $(N-H)_{bonded}$. IR ($CHCl_3$, cm^{-1}): 1671 (CO). ^{1}H-NMR (DMSO-d_6, ppm): 1.76, 2.46, 2.50, 2.82, 3.30 ($-CH_2-$); 5.81 (−NH−); 1.42, 1.65 (−SH).

Mo[BH(Me$_2$pz)$_3$](NO)I$_2$. This compound was synthesized and characterized by previously published methods.[13]

Mo[BH(Me$_2$pz)$_3$](NO)[S(CH$_2$)$_2$CONH(CH$_2$)$_2$S] (1). Sodium methoxide (3.84 g, 71.2 mmol) and the dithiol $HS(CH_2)_2CONH(CH_2)_2SH$ (11.75 g, 71.2 mmol) were combined in MeOH (100 mL) and stirred for 1 h. The solvent was removed by evaporation under vacuum on a hot water bath. THF (200 mL) was then added, and the resulting slurry was stirred overnight. The liquid was decanted and the solid, $Na_2[S(CH_2)_2CONH(CH_2)_2S]$, was dried under vacuum. $Mo[BH(Me_2pz)_3](NO)I_2$ (1.20 g, 1.56 mmol) and $Na_2[S(CH_2)_2CONH(CH_2)_2S]$ (0.326 g, 1.56 mmol) were mixed in THF (150 mL) and refluxed for 2 days. The solvent was removed by evaporation under vacuum, and the crude product, **1**, was redissolved in $CHCl_3$ (30 mL) and filtered to remove NaI. Chloroform was then removed by evaporation under vacuum leaving a dark brown powder. The product was purified by column chromatography on silica gel using 10% THF/$CHCl_3$. The desired fraction was eluted as a red band. UV−vis ($CHCl_3$, nm): 362, 476. The purified product was obtained from this solution as dark red crystals by the addition of hexane to a saturated solution (yield: 0.180 g, 19.4%). Crystals suitable for single crystal X-ray crystallography and elemental analysis were grown by the slow addition of hexane to a saturated solution of **1** in CH_2Cl_2. Anal. Calcd for $C_{20}H_{31}BMoN_8O_2S_2{\cdot}H_2O$ (**1**): C, 39.75; H, 5.50; N, 18.54. Found: C, 40.58; H, 5.29; N, 18.84.

Mo[BH(Me$_2$pz)$_3$](NO)[S(CH$_2$)$_n$S] (2 (*n* = 5), 3 (*n* = 6)). Compounds **2** and **3** were synthesized from the appropriate ligand precursors $HS(CH_2)_nSH$, $n = 5$ and 6 (Aldrich Chemical Co.) by the methods employed in the synthesis of **1** (yield: 18.4% for **2** and 27.8% for **3**). Anal. Calcd for $C_{20}H_{32}BMoN_7OS_2{\cdot}0.5CH_2C_{12}$ (**2**): C, 41.04; H, 5.54; N, 16.34. Found: C, 41.25; H, 5.57; N, 15.75. Anal. Calcd for $C_{21}H_{34}BMoN_7OS_2{\cdot}0.4C_6H_{14}$ (**3**): C, 46.39; H, 7.04; N, 16.19. Found: C, 46.42; H, 6.85; N, 16.22.

Proton NMR data were collected by using Varian Gemini-200 and General Electric QE-300 spectrometers.

IR data were collected at 4 cm^{-1} resolution using a 5 mm path length cell with a Nicolet 5DXB spectrometer. All samples were prepared in $CDCl_3$. Resonance Raman data were collected at room temperature with 10 cm^{-1} spectral slit width at a scan rate of 5 s/cm^{-1}. Samples were prepared as saturated CH_2Cl_2 solutions and were irradiated in backscattering geometry in a spinning 8 in. ultrathin-walled NMR tubes (Wilmad).[16] A description of the experimental apparatus and data processing software has been previously provided.[17]

Electronic absorption data were obtained using a Hewlett-Packard 8452A diode array spectrometer.

Elemental analyses were performed by Galbraith Laboratories, Inc., Knoxville, TN.

Table 1. Crystallographic data for Mo[BH(Me$_2$pz)$_3$](NO)[S(CH$_2$)$_2$CONH(CH$_2$)$_2$S] (**1**)

chem formula	$C_{20}H_{31}BMoN_8O_3S_2$
fw	602.40
space group	$P2_1/c$
a, Å	11.878(2)
b, Å	10.804(1)
c, Å	21.453(4)
β, deg	105.54
V, Å^3	2652.4(7)
Z	4
T, K	293
λ, Å	0.710 73
cryst system	monoclinic
ϱ_{calcd}, g·cm^{-3}	1.509
μ, mm^{-1}	0.690
cryst size, mm	0.22 × 0.40 × 0.48
2θ limit, deg	$4 < 2\theta < 48$
no. of rflns collcd	4311
no. of indep rflns	4191
GOF	0.993
final R indices [$I > 2\sigma(I)$]	$R1 = 0.0374$, w$R2 = 0.0936$
R indices (all data)	$R1 = 0.0491$, w$R2 = 0.0985$
$\Delta(\varrho)$, e Å^{-3}	+0.884, −0.400

Table 2. Selected Bond Lengths and Angles for Mo[BH(Me$_2$pz)$_3$](NO)[S(CH$_2$)$_2$CONH(CH$_2$)$_2$S] (**1**)

Bond Distances (Å)			
Mo−S(1)	2.343(1)	Mo−N(7)	1.767(4)
Mo−S(2)	2.353(1)	S(1)−C(20)	1.826(5)
Mo−N(1)	2.249(3)	S(2)−C(16)	1.825(4)
Mo−N(3)	2.233(3)	O(1)−N(7)	1.199(4)
Mo−N(5)	2.229(3)		
Bond Angles (deg)			
N(7)−Mo−N(5)	96.77(14)	N(7)−Mo−N(3)	97.76(14)
N(5)−Mo−N(3)	76.26(12)	N(7)−Mo−N(1)	176.33(13)
N(5)−Mo−N(1)	86.22(12)	N(3)−Mo−N(1)	85.00(11)
N(7)−Mo−S(1)	92.89(12)	N(5)−Mo−S(1)	163.39(9)
N(3)−Mo−S(1)	89.09(9)	N(1)−Mo−S(1)	84.71(9)
N(7)−Mo−S(2)	94.98(11)	N(5)−Mo−S(2)	87.50(8)
N(3)−Mo−S(2)	160.39(9)	N(1)−Mo−S(2)	83.00(8)
S(1)−Mo−S(2)	105.13(4)		

Cyclic voltammetry was carried out with a Pine Instruments AFRDF4 potentiostat. The measurements were made in dry acetonitrile, under N_2 in a Vacuum Atmospheres glovebox.

X-ray Structure Determination. Crystallographic data for **1** are listed in Table 1, and selected bond lengths and angles are presented in Table 2. Photographic evidence and systematic absences in the diffraction data allowed a unique space group assignment. Azimuthal scans about the diffraction vector showed a variation of less than 10%, and a correction for absorption was neglected. The structure was solved from a Patterson map. All non-hydrogen atoms were anisotropically refined, and hydrogen atoms (except for those on the water molecule which were ignored) were treated as idealized contributions. All computations used the routines of SHELX-93 and SHELXTL (G. Sheldrick, Siemens XRD, Madison, WI).

Results and Discussion

Selected bond lengths for **1** (Figure 1) (Tables 1 and 2) are Mo−N$_{pz}$(avg) = 2.237(3), Mo−NO = 1.767(4), Mo−S(1) = 2.343(1) and Mo−S(2) = 2.353(1) Å. These bond lengths are similar to those observed in the monodentate thiolate complexes $Mo[HB(Me_2pz)_3](NO)(SR)_2$, R = C_6H_5 and $(CH_2)_mCONHCH_3$, $m = 1$ and 2.[12,18] In the solid state the amide group of **1** resides in a plane that is roughly parallel to the S(1), S(2), NO face. The complex has dihedral angles of −6.2° [N(7)−Mo−S(1)−C(20)] and 9.7° [N(7)−Mo−S(2)−C(16)], nearly identical to those observed in the related monodentate dithiolate com-

---

(16) Walters, M. A. *Appl. Spectrosc.* **1983**, *37*, 299−300.

(17) Chung, W. P.; Dewan, J. C.; Walters, M. A. *J. Am. Chem. Soc.* **1991**, *113*, 525−530.

(18) Roberts, S. A.; Enemark, J. H. *Acta Crystallogr.* **1989**, *C45*, 1292−1294.

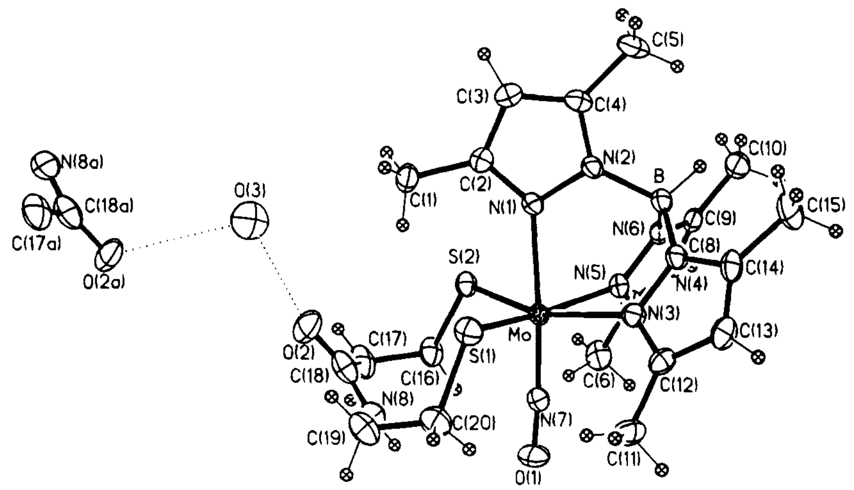

Figure 1. Molecular structure of Mo[BH(Me$_2$pz)$_3$](NO)[S(CH$_2$)$_2$CONH(CH$_2$)$_2$S]·H$_2$O, **1**, containing a fragment of an adjacent hydrogen-bonded molecule. Atoms are shown as 30% probability ellipsoids.

Table 3. Cyclic Voltammetry, and Raman Spectroscopic Results for Mo[HB(Me$_2$pz)$_3$](NO)(SRS), $E_{1/2}$,[a] ΔE,[b] and ν(NO)[c]

[SRS]$^{2-}$ group (compd no.)	$E_{1/2}$, V	ΔE, mV	ν(NO), cm^{-1}
[S(CH$_2$)$_2$CONH(CH$_2$)$_2$S]$^{2-}$ (**1**)	−0.793	65	1667
[S(CH$_2$)$_5$S]$^{2-}$ (**2**)	−0.930	100	1659
[S(CH$_2$)$_6$S]$^{2-}$ (**3**)	−1.013	75	1656

[a] All data were acquired in CH$_3$CN at a scan rate of 50 mV/s with Et$_4$NClO$_4$ (0.10 M) as electrolyte. Electrodes: working electrode, glassy carbon; counter electrode, Pt wire; reference electrode, saturated calomel. $E_{1/2}$(ferrocene) vs SCE: +0.380 V in CH$_3$CN. [b] ΔE is the peak-to-peak separation of the cathodic and anodic peaks. ΔE(ferrocene) = 80 mV in CH$_3$CN. [c] These frequencies are reported relative to $\nu_2(a_1)$, the deformation band of CH$_2$Cl$_2$, which we assign to a peak at 1425 cm^{-1}. Raman data were acquired in CH$_2$Cl$_2$ using 488.0 nm, 100 mW excitation in the backscattering geometry, with a 10 cm^{-1} slit width.

plexes.[12] These dihedral angles correlate with good d(Mo)−p(S) orbital overlap.[18,19]

Amide−thiolate nonbonded distances of **1** in the solid state are large, N(8)···S(1) = 3.297 and N(8)···S(2) = 3.642 Å. Therefore, in the crystal, neither the orientation nor the distances between the amide N−H and thiolate sulfur atoms are suitable for N−H···S hydrogen bond formation. Solution infrared data acquired in CDCl$_3$ show two amide N−H stretching, ν(NH), peaks, at 3434 and 3308 cm^{-1}. These bands belong to non-hydrogen-bonded (free) and hydrogen-bonded (bonded) N−H groups, respectively. The intensity of the $\nu(\mathrm{NH})_{\mathrm{free}}$ band at 3434 cm^{-1} relative to ν(NH) of *N*-methylmercaptopropionamide (which does not form intramolecular N−H···S hydrogen bonds[20−22]) is consistent with a room-temperature equilibrium constant of $K = [\mathrm{NH_{bonded}}]/[\mathrm{NH_{free}}] = 6.7$. Although we observe a water of crystallization, the peak at 3308 cm^{-1} does not result from N−H group hydrogen bonding to water. The addition of water to CHCl$_3$ to the point of saturation has no effect on ν(NH) of the secondary amide *N*-methylmercaptopropionamide. The solution data therefore indicate that the amide group has reoriented so as to allow the formation of one or two N−H···S hydrogen bonds.

The conformational change that would be required for the amide N−H group to form an intramolecular hydrogen bond probably involves a rotation of the amide group about the C(17)−C(18) and N(8)−C(19) bonds. A qualitative study of amide reorientation in **1** suggests that two contacts would occur between N−H and S at distances of approximately 2.8 Å for N(8)···S(1) and 2.9 Å for N(8)···S(2). Distances such as these have been observed in bent N−H···S hydrogen bonds such as those in *o*-amino thiolate [SC$_6$H$_4$NH$_2$]$^-$ and *o*-amido thiolate [SC$_6$H$_4$NHCOR]$^-$ ligands.[5,8,23] The formation of an amide−nitrosyl hydrogen bond is precluded by the large distance between the two groups. Therefore, we conclude that the vibrational spectroscopic data on the N−H group are consistent with the formation of two intramolecular N−H···S hydrogen bonds in solution as represented below:

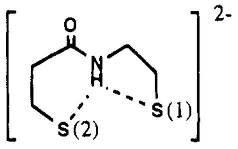

The Mo(II)/Mo(III) redox potentials of **1**−**3** as measured in CH$_3$CN are shown in Table 3. In complex **1**, the presence of an amide group close to sulfur results in a redox potential of −0.793 V. As expected, this potential is positive relative to those of **2** and **3**, which are −0.930 and −1.013 V, respectively. A similar observation was made earlier for the series of complexes Mo[HB(Me$_2$pz)$_3$](NO)(SR)$_2$, R = (CH$_2$)$_n$CONR′CH$_3$, n = 1 and 2, and R′ = H and CH$_3$, where N−H···S hydrogen bonds were shown to induce a large positive shift in redox potential.[12] The difference in the redox potentials of **2** and **3** may be accounted for by their respective ON−Mo−S−C dihedral angles.[15] However, the differences between the redox potential of **1** and those of the complexes Mo[HB(Me$_2$pz)$_3$](NO)(SR)$_2$, R = (CH$_2$)$_n$CONHCH$_3$, n = 1 and 2, all of which have nearly identical ON−Mo−S−C dihedral angles, are likely due to both the nature of the N−H···S bonds and to charge−dipole interactions.[12]

The nitrosyl stretching frequencies, ν(NO), of **1**−**3** (Table 3) reflect differences among the complexes in their electron densities at Mo. Therefore these frequencies can be used to monitor the effects of N−H···S hydrogen bonding, which have been shown to cause a decrease in electron density at Mo in the complex Mo[HB(Me$_2$pz)$_3$](NO)(SCH$_2$CONHCH$_3$)$_2$ relative

---

(19) Ashby, M. T.; Enemark, J. H. *J. Am. Chem. Soc.* **1986**, *108*, 730−733.

(20) Zuppiroli, G.; Perchard, C.; Baron, M. H.; de Loze, C. *J. Mol. Struct.* **1980**, *69*, 1−16.

(21) Perchard, C.; Zuppiroli, G.; Gouzerh, P.; Jeannin, Y.; Robert, F. *J. Mol. Struct.* **1981**, *72*, 119−129.

(22) Zuppiroli, G.; Perchard, C.; Baron, M. H.; de Loze, C. *J. Mol. Struct.* **1981**, *72*, 131−141.

(23) Okamura, T.-a.; Ueyama, N.; Nakamura, A.; Ainscough, E. W.; Brodie, A. M.; Waters, J. M. *J. Chem. Soc., Chem. Commun.* **1992**, 1658−1660.

to non-hydrogen-bonding complexes.[12] Infrared data recorded in chloroform reveals ν(NO) peaks at 1679, 1657, and 1651 cm^{-1} for **1**–**3**, respectively. The 1679 cm^{-1} peak of **1** is actually a composite of peaks belonging to ν(NO) and ν(CO). We employed resonance Raman spectroscopy to locate ν(NO) by the resonance enhancement of its intensity relative to that of ν(CO). The ν(NO) frequencies for **1**–**3** were measured using 488.0 nm excitation, in methylene chloride, which has a useful marker band at 1425 cm^{-1}. The ν(NO) peaks appear at 1667 (**1**), 1659 (**2**), and 1656 (**3**) cm^{-1} (Table 3). There is a significant decrease in the frequency of ν(NO) in conjunction with decreasing redox potential. The relationship observed here between ν(NO) and $E_{1/2}$ is in accord with earlier observations on related Mo–hydrotris(pyrazolyl)borato compounds.[12,24] These data provide further evidence of hydrogen bonding-induced electron withdrawal from the Mo(III) ion via coordinated sulfur. This process results in a decrease in π-back-bonding to NO and causes an increase in ν(NO).

The synthesis and characterization of complex **1** represents a particularly useful approach to the study of hydrogen bond and/or dipolar effects on redox potentials in metal complexes. The linkage of the amide group to sulfur by an alkyl chain ensures that inductive effects on sulfur are cut off.[25] Relative to the monodentate Mo thiolate complexes discussed above, incorporation of the amide group in the bidentate alkanethiolate ligand effects greater control over the *distance* of the amide from the metal–sulfur coordination sphere. This control does not extend to the *orientation* of the amide group which appears to rotate about the C(17)–C(18) and N(8)–C(19) bonds. However the redox potential and ν(NO) frequency shifts of **1**, relative to those of **2** and **3**, indicate a dynamically averaged effect of the amide group on the electronic characteristics of the Mo coordination sphere.

As shown earlier,[26] the $\{Mo[BH(Me_2pz)_3]\}^{2+}$ group forms particularly stable dithiolate adducts and is therefore a convenient molecular platform on which to investigate amide group interactions with coordinated sulfur in solution. The variety of influences on redox potential at a coordination site, with a fixed set of components, is becoming increasingly evident on the basis of results with this model system. Thus far, in the molybdenum thiolate complexes, these influences have been shown to include (i) Mo–S d–p bonding,[15] (ii) charge–dipole electrostatic effects, and (iii) N–H··S bonding.[12] The last of these conclusions is based on a model system that avoids the use of π-conjugated ligands while maintaining good amide–thiolate proximity. This type of molecule and the resulting data represent an important advance in the study of N–H··S hydrogen bonds in metal–thiolate complexes.

Acknowledgment. This investigation has been supported by grants from the EXXON Education Foundation and the National Science Foundation (Grant No. CHE-9203455) to M.A.W.

Supplementary Material Available: Tables of complete data collection information, atomic coordinates and *U* values, bond distances, bond angles, anisotropic thermal parameters, and positional and thermal parameters of the H atoms for **1** and a stereo packing diagram (7 pages). Ordering information is given on any current masthead page.

IC941209E

---

(24) Obaidi, N. A.; Chaudhury, M.; Clague, D.; Jones, C. J.; Pearson, J. C.; McCleverty, J. A.; Salam, S. S. *J. Chem. Soc., Dalton Trans.* **1987**, 1733–1736.

(25) Bowden, K. *J. Chim. Phys.* **1992**, *89*, 1647–1659.

(26) McCleverty, J. A.; Drane, A. S.; Bailey, N. A.; Smith, J. M. A. *J. Chem. Soc., Dalton Trans.* **1983**, 91–96.